Energy-dispersive neutron imaging and diffraction of magnetically driven twins in a Ni_2MnGa single crystal magnetic shape memory alloy

Saurabh Kabra[1], Joe Kelleher[1], Winfried Kockelmann[1], Matthias Gutmann[1], Anton Tremsin[2]

[1] Rutherford Appleton Laboratory, ISIS Facility, Chilton, OX11 0QX, UK

[2] Space Sciences Laboratory, University of California, Berkeley, CA 94720, USA

saurabh.kabra@stfc.ac.uk

Abstract. Single crystals of a partially twinned magnetic shape memory alloy, Ni_2MnGa, were imaged using neutron diffraction and energy-resolved imaging techniques at the ISIS spallation neutron source. Single crystal neutron diffraction showed that the crystal produces two twin variants with a specific crystallographic relationship. Transmission images were captured using a time of flight MCP/Timepix neutron counting detector. The twinned and untwinned regions were clearly distinguishable in images corresponding to narrow-energy transmission images. Further, the spatially-resolved transmission spectra were used to elucidate the orientations of the crystallites in the different volumes of the crystal.

1. Introduction

Large actuation strains, at least an order of magnitude higher than magnetostrictive materials [1], can be achieved in the class of materials known collectively as “magnetic shape memory alloys”. The interplay between the high temperature cubic phase and low temperature monoclinic/tetragonal phase (with several twin variants) can be exploited in these alloys to achieve large reversible strains in the stress-temperature-field (magnetic) space. The most successful system in this class of alloys has been the Heusler alloy, Ni_2MnGa, which has been studied as the subject of this article. We have used neutron imaging and diffraction to study twin variants in the low temperature monoclinic phase (so called ‘martensite’) in single crystalline samples of Ni_2MnGa. The monocrystals have a modulated ordered monoclinic crystal structure at room temperature [2]. The cell angles are close to 90 degrees, making the tetragonal assumption reasonable in many cases.

Owing to a very low twinning stress, the application of an external magnetic field (<0.5 T) is sufficient to twin the crystal into another orientation. As the orientation of the twin variants is different, so is the magnetization direction [3][4]. Therefore, as the field direction is changed, a different twin variant is formed. This is illustrated in figure 1(a) which shows that the twins prefer the crystal c-axis parallel to the externally applied magnetic field. These twins grow and eventually the

entire crystal is transformed into the new twinned variant, if a strong enough (>0.65 T) external field is applied.

In this study, we have used single crystal neutron diffraction to find the relative orientations of the twinned crystals and neutron imaging to resolve the morphology of the twins and the untwinned material. Given that these were bulk crystals (several millimetres) neutron methods proved ideal to study them owing to high neutron penetration. Neutron imaging with a high-resolution neutron imaging detector was performed in time of flight (TOF) mode to discriminate the energies of the neutrons. This not only helped in enhancing the contrast between the twins but also the full energy dispersive spectra obtained could be used for further analysis of spatially resolved orientations, strains etc.

2. Experiments and data analysis

2.1. Sample history

Single crystals of Ni_2MnGa with a 5M modulation along the c-axis were obtained from Adaptamat Ltd.[5]. The composition of the samples was 50at.%Ni, 28.5at.%Mn and 21.5at.%Ga and the martensitic transformation temperature was ~50^{o}C. The cuboid crystals were 5 x 5 x 15 mm in size, with the {100} axis along the length of the crystal and the other two crystallographic axis roughly along the remaining edges. Parts of the samples were exposed to an external magnetic field using a Neodymium based permanent magnet. This introduced a region in the crystal which was twinned with respect to the rest of the original crystal. The magnetic field was subsequently removed and the partially twinned system was used for neutron experiments. The removal of the field, did not de-twin the crystal as twinning is not reversible in these materials without the application of an external field or stress.

2.2. Single crystal neutron diffraction

The crystals were measured on the SXD [6] instrument at the ISIS neutron source. The crystals were exposed to the neutron beam for ~20 minutes. The beam size was greater than the sample dimensions and therefore the entire sample including the original crystal and the twin contributed towards the detected signal. SXD comprises of 11 position sensitive detector panels which subtends a large solid angle on to the sample resulting in a large number of diffraction spots to be utilized. Automated peak and cell finding was achieved using the SXD2001 software [7] starting with an initial cell reported in [2]. Two distinct crystalline orientations were found using the automated algorithm. Figure 1(b) shows the orientation relation between the two crystalline orientations that were found using the SXD data. The atomic positions shown in the figure were from the reported crystal structure in reference [2] and were not refined. The orientation of the twin is essentially a ~90 degree rotation about the b-axis of the original crystal thereby swapping the directions of the a-axis and c-axis.

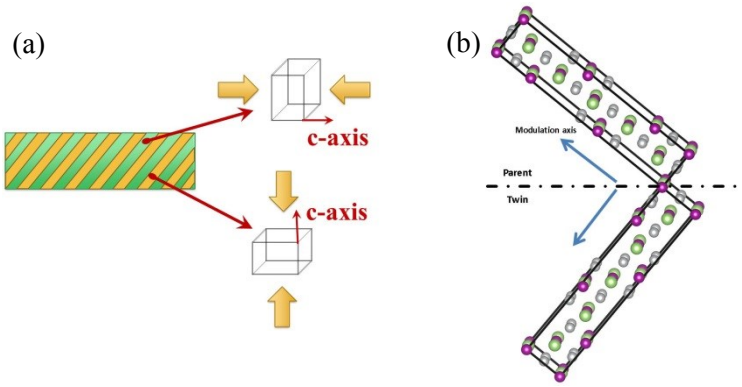

Figure 1. (a) Schematic diagram showing how different parts of the crystal transform to different twin variants as the applied field direction is varied. (b) Schematic diagram showing the orientation relation between the two twin variants obtained from the neutron diffraction analysis.

2.3. Neutron Imaging

Imaging experiments were performed on the ROTAX [8] test beamline at the ISIS neutron source. Simple transmission geometry was used with the sample placed between the beam and the detector (figure 2). The area detector was placed nominally perpendicular to the beam and the sample was placed ~12 mm to the detector active area. The b-axis of the original (untwinned) crystal was approximately parallel to the beam.

The MCP/Timepix detector (figure 2) used for the imaging experiments [9],[10] allowed measurement of the neutron energy for each detected particle. The position of each neutron was detected with the accuracy of 55 μm (current detector pixel size) and timing binning of 20 μs for thermal and cold neutrons. Multiple frames where acquired for each neutron pulse. The acquisition system was synchronized with the trigger of the neutron source, providing the possibility to calculate the energy of each neutron from its time of flight. The active area of the detector was 28x28 mm^2, defined by the 2x2 array of Timepix readout ASICs, developed by the Medipix collaboration [11]. The neutrons arriving at the active area of the detector are converted into an electron cloud by the neutron sensitive microchannel plates, manufactured by Nova Scientific. Each neutron produces ~10^4-10^5 electrons, thus enabling operation with no readout noise. This detector will be used as a standard equipment on the IMAT imaging beamline [12].

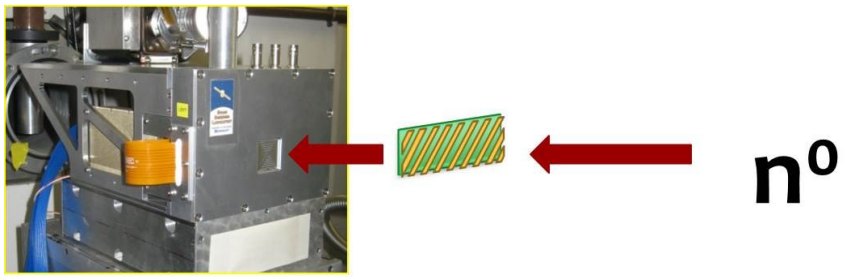

Figure 2. Geometry of the neutron imaging experiment. The sample was mounted close (few mm) to the neutron window of the detector head.

The imaging measurement resulted in a stack of images of dimensions 512 x 512 pixels each. Every image represented a time of flight bin which was later converted to wavelength. Thus the transmission spectra consisting of several thousand energy bins was measured for each pixel of the

data set, all in one experiment. An open beam measurement (without any sample) was also carried out under the same setup. This was used to normalize the data both for the flux distribution as a function of TOF and for spatial non-uniformity (combination of beam non-uniformity and pixel sensitivity). Figure 3(a) shows the white beam radiograph of the twinned crystal where all energies have been summed up. No apparent contrast can be inferred. Figure 3(b) shows a corresponding image where only the neutrons in the range of 2.7-2.8 Å have been summed. The twin (yellow-green region) and original crystal (blue region) are easily distinguishable in this image. The neutron intensities as a function of wavelength have been plotted in figure 3(c). The colored dots on 3(b) indicate both locations and the color of the corresponding plots.

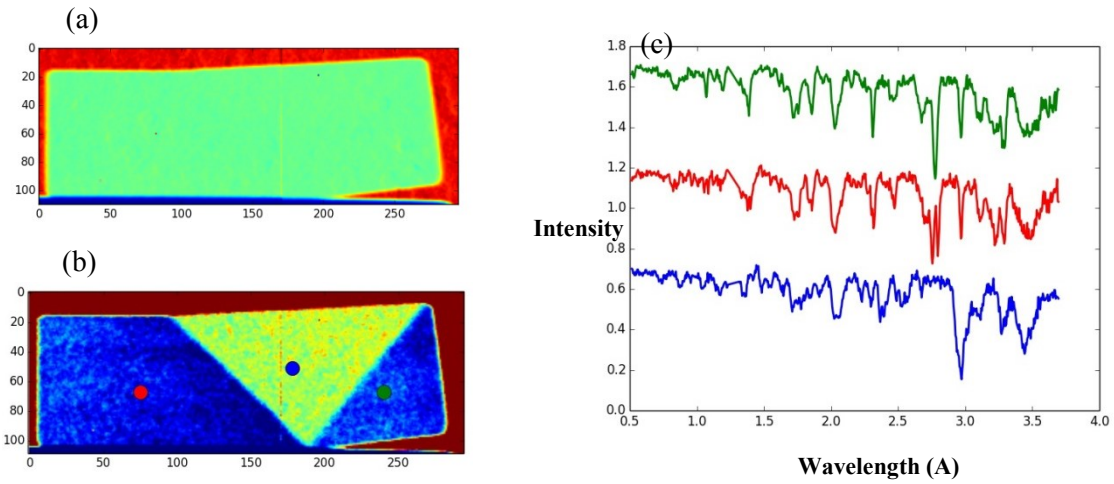

Figure 3. (a) White beam transmission image of the twinned crystal. (b) Radiograph using a limited range of neutron energies showing contrast between original crystal and twin. (c) Transmission spectra from the different regions of the original and twinned crystals (the dots on fig b correspond to regions sampled and colour of the dot corresponds to the colour of the curve)

3. Results and discussion

It is evident from Figure 3 that, by limiting the energy range of the imaging data, contrast can be enhanced between the differently oriented parts of the crystals. The reason for this is that different crystal orientations with respect to the beam results in Bragg condition being satisfied for different sets of crystalline planes. The corresponding neutrons that have diffracted are missing in the transmitted beam and therefore the characteristic 'dips' occur in the transmission spectra (figure 3(c)). Both the intensities and the positions of these dips are related to the orientation of the crystals. Markedly, in figure 3(c), the red and the green plots look quite similar as compared to the blue plot which is quite different from both. This is not surprising, given that the blue plot is from the twinned region of the crystal, while both red and green plot are from the original crystal regions. The two original crystal regions do show some differences because of slight mis-orientation between them arising due to the triangular shape of the twin.

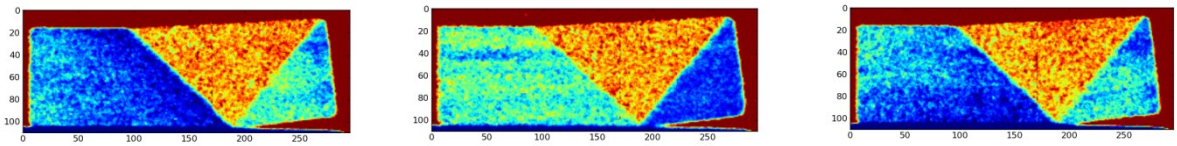

Figure 4. Radiographs of the twinned crystals with various energy ranges showing mosaic features in the original crystal.

Figure 4 shows the radiographs of the twinned crystals at several chosen energy ranges. The figure clearly shows various linear features running along the length of the crystal in the original crystal. These linear features on the single crystal are along the growth direction of the single crystal. It can be speculated that these are probably due to slight misalignments between subdomains during the growth process.

For future work, the authors plan to study the dynamics of the twinning in these crystals by subjecting the crystals to a cyclic magnetic field in situ. These stroboscopic experiments will shed light on the twin kinetics and the dependence of twin morphology on external parameters such as frequency of rotation and the strength of field.

4. Conclusions

Single crystals of Ni_2MnGa can spontaneously twin upon the application of an external magnetic field. Neutrons are an ideal tool to study these twinned crystals due to their high penetration capability and high coherent cross section for this material. Single crystal diffraction shows the orientation relation between the untwinned and the twinned regions while high resolution energy dispersed neutron imaging shows the morphology of the twinned regions. Further, the mosaic microstructure of the original crystal was elucidated during the imaging experiments.

References

[1] Ullakko K, Huang J K, Kantner C, O'Handley R C and Kokorin V V. 1996 Large magnetic-field-induced strains in Ni2MnGa single crystals *Appl. Phys. Lett.* **69** 1966

[2] Righi L, Albertini F, Pareti L, Paoluzi A and Calestani G 2007 Commensurate and incommensurate "5M" modulated crystal structures in Ni–Mn–Ga martensitic phases *Acta Mater.* **55** 5237–45

[3] Karaca H, Karaman I, Basaran B, Chumlyakov Y and Maier H 2006 Magnetic field and stress induced martensite reorientation in NiMnGa ferromagnetic shape memory alloy single crystals *Acta Mater.* **54** 233–45

[4] Lai Y W, Scheerbaum N, Hinz D, Gutfleisch O, Schäfer R, Schultz L and McCord J 2007 Absence of magnetic domain wall motion during magnetic field induced twin boundary motion in bulk magnetic shape memory alloys *Appl. Phys. Lett.* **90** 192504

[5] Tellinen J, Suorsa I, Jaaskelainen A, Aaltio I and Ullkko K 2002 Basic properties of magnetic shape memory actuators *Actuator 2002, Wirtschaftsfoerderung Bremen GmbH, Bremen* pp 566–9

[6] Keen D A, Gutmann M J and Wilson C C 2006 SXD – the single-crystal diffractometer at the ISIS spallation neutron source *J. Appl. Crystallogr.* **39** 714–22

[7] Gutmann M J 2005 No Title *SXD2001,. ISIS Facil. Rutherford Applet. Lab. Oxfordshire, Engl.*

[8] Kockelmann W A, Weisser M, Heinen H, Kirfel A and Schäfer W 2000 Application Spectrum and Data Quality of the Time-to-Flight Neutron Diffractometer ROTAX at ISIS *Mater. Sci. Forum* **321-324** 332–7

[9] Tremsin A S 2012 High resolution neutron counting detectors with microchannel plates and their applications in neutron radiography, diffraction and resonance absorption imaging *Neutron News* **23** 35–8

[10] Tremsin A S, Vallerga J V, McPhate J B and Siegmund O H W 2015 Optimization of high count rate event counting detector with Microchannel Plates and quad Timepix readout *Nucl. Instruments Methods Phys. Res. Sect. A Accel. Spectrometers, Detect. Assoc. Equip.* **787** 20–5

[11] Llopart X, Ballabriga R, Campbell M, Tlustos L and Wong W 2007 Timepix, a 65k programmable pixel readout chip for arrival time, energy and/or photon counting measurements *Nucl. Instruments Methods Phys. Res. Sect. A Accel. Spectrometers, Detect. Assoc. Equip.* **581** 485–94

[12] Kockelmann W, Burca G, Kelleher J F, Kabra S, Zhang S-Y, Rhodes N J, Schooneveld E M, Sykora J, Pooley D E, Nightingale J B, Aliotta F, Ponterio R C, Salvato G, Tresoldi D, Vasi C, McPhate J B and Tremsin A S 2015 Status of the Neutron Imaging and Diffraction Instrument IMAT *Phys. Procedia* **69** 71–8